



Stem cell-based gene therapy activated using magnetic hyperthermia to enhance the treatment of cancer



Perry T. Yin ^a, Shreyas Shah ^b, Nicholas J. Pasquale ^b, Olga B. Garbuzenko ^c,
Tamara Minko ^{c, d}, Ki-Bum Lee ^{a, b, *, 1}

^a Department of Biomedical Engineering, Rutgers, The State University of New Jersey, Piscataway, NJ, 08854, USA

^b Department of Chemistry and Chemical Biology, Rutgers, The State University of New Jersey, Piscataway, NJ, 08854, USA

^c Department of Pharmaceutics, Rutgers, The State University of New Jersey, Piscataway, NJ, 08854, USA

^d Rutgers Cancer Institute of New Jersey, New Brunswick, NJ, 08903, USA

ARTICLE INFO

Article history:

Received 9 November 2015

Accepted 10 November 2015

Available online 12 November 2015

Keywords:

Magnetic core–shell nanoparticles

Hyperthermia

Stem cell therapy

Gene therapy

Cancer therapy

ABSTRACT

Stem cell-based gene therapies, wherein stem cells are genetically engineered to express therapeutic molecules, have shown tremendous potential for cancer applications owing to their innate ability to home to tumors. However, traditional stem cell-based gene therapies are hampered by our current inability to control when the therapeutic genes are actually turned on, thereby resulting in detrimental side effects. Here, we report the novel application of magnetic core–shell nanoparticles for the dual purpose of delivering and activating a heat-inducible gene vector that encodes TNF-related apoptosis-inducing ligand (TRAIL) in adipose-derived mesenchymal stem cells (AD-MSCs). By combining the tumor tropism of the AD-MSCs with the spatiotemporal MCNP-based delivery and activation of TRAIL expression, this platform provides an attractive means with which to enhance our control over the activation of stem cell-based gene therapies. In particular, we found that these engineered AD-MSCs retained their innate ability to proliferate, differentiate, and, most importantly, home to tumors, making them ideal cellular carriers. Moreover, exposure of the engineered AD-MSCs to mild magnetic hyperthermia resulted in the selective expression of TRAIL from the engineered AD-MSCs and, as a result, induced significant ovarian cancer cell death *in vitro* and *in vivo*.

© 2015 Elsevier Ltd. All rights reserved.

1. Introduction

Ovarian cancer currently ranks fifth in cancer mortalities among women and is the leading cause of death from gynecological malignancies [1]. The conventional mode of therapy for this cancer consists of cytoreductive surgery, followed by adjuvant platinum/taxane-based chemotherapy [2]. However, while most ovarian cancer patients exhibit initial sensitivity to chemotherapy, over 70% of these patients are diagnosed at an advanced stage, when the tumors have already metastasized throughout the peritoneal cavity [3]. As a consequence, the majority of ovarian cancer patients experience recurrence within 18–24 months of treatment and only 20% of them survive longer than 5 years after

their initial diagnosis [4].

To enhance the treatment of advanced cancers, such as advanced ovarian cancer, mesenchymal stem cell (MSC)-based therapies have emerged as an attractive alternative that can overcome the limited tumor-targeting ability of conventional treatments [5]. MSCs have the intrinsic ability to self-renew and differentiate into multiple lineages including osteoblasts, chondrocytes, and adipocytes [6]. More importantly, several groups have demonstrated that these stem cells have the innate ability to migrate to tumors including ovarian tumors/metastases, even following systemic administration [7–10]. While the exact mechanism is still being elucidated, this tumor tropism has prompted the development of stem cell-based gene therapies, wherein MSCs are genetically engineered to express therapeutic molecules and therefore, act as targeted delivery vehicles to enhance our ability to treat metastatic cancers [11,12].

To this end, a number of therapeutic molecules have been investigated, including direct effectors of apoptosis, such as the cytokines, interferon- β (IFN- β) [13], and tumor necrosis factor-

* Corresponding author. Department of Biomedical Engineering, Rutgers, The State University of New Jersey, Piscataway, NJ, 08854, USA

E-mail address: kblee@rutgers.edu (K.-B. Lee).

¹ Website: <http://kblee.rutgers.edu>.

related apoptosis inducing ligand (TRAIL) [14], as well as more indirect immunomodulatory molecules like interleukin 12 (IL-12) [15]. Of these, TRAIL is a particularly attractive therapeutic candidate owing to its ability to selectively induce apoptosis in malignant cells, but not in most normal cells [16]. For example, Mueller et al. reported that multipotent MSCs that were genetically engineered to express TRAIL were able to induce apoptosis and inhibit the growth of colorectal carcinoma cells *in vivo* with no serious observable side effects [17]. Similarly, Loebinger and colleagues demonstrated that MSCs engineered to produce and deliver TRAIL could induce apoptosis in lung, breast, squamous, and cervical cancer cells [14]. Importantly, these engineered MSCs were able to significantly reduce tumor growth in a subcutaneous breast cancer xenograft and could home to and reduce lung metastasis. However, while TRAIL has largely been demonstrated to be biocompatible with normal cells, there have been a number of reports indicating potential hepatotoxicity upon treatment with TRAIL, thereby greatly dampening its clinical potential [18,19]. As such, to limit these potentially detrimental side effects and in order for stem cell therapies to reach their full potential, there remains a pressing need for approaches that can allow for the precise spatiotemporal control of therapeutic gene activation such that the engineered stem cells only express their therapeutic payload once they have reached the targeted tumor sites.

Herein, we report the novel application of magnetic core–shell nanoparticles (MCNPs), composed of a highly magnetic zinc-doped iron oxide (ZnFe_2O_4) core and a biocompatible mesoporous silica (mSi) shell, for the dual purpose of delivering and activating a heat-inducible gene vector that encodes a secretable form of TRAIL in MSCs (Fig. 1). For this purpose, we developed a plasmid with the heat shock protein 70B' (HSP70B') promoter (Fig. 1B), which has previously been demonstrated to be more heat-specific than other heat shock promoters [20]. As such, the MSCs can first be engineered with MCNPs that are complexed with the heat-inducible TRAIL plasmid *in vitro*. Afterwards, following *in vivo* injection and

migration of the engineered MSCs to the targeted tumor sites, TRAIL expression can be specifically activated via the induction of mild magnetic hyperthermia ($\sim 41^\circ\text{C}$). In this report, we demonstrated the efficient and biocompatible uptake of MCNP–plasmid complexes into MSCs. In particular, we observed that the engineering process had no significant effects on MSC proliferation or differentiation. Moreover, the engineered MSCs retained their tumor tropism towards disseminated peritoneal ovarian cancer xenografts. Importantly, we demonstrated that mild magnetic hyperthermia, via exposure of the engineered MSCs to an alternating magnetic field (AMF), could be used to specifically raise the intracellular temperature to $\sim 41^\circ\text{C}$, which resulted in the selective expression of TRAIL in the engineered MSCs. As a result, significant ovarian cancer cell apoptosis and death was observed *in vitro* and *in vivo*. Overall, by combining the tumor tropism of MSCs with the spatiotemporal MCNP-based delivery and activation of TRAIL expression, this platform provides an attractive means with which to enhance our control over the activation of stem cell-based gene therapies.

2. Materials and methods

2.1. Nanoparticle synthesis and characterization

The synthesis of ZnFe_2O_4 magnetic nanoparticles (MNPs) has previously been reported and modified by our group [21–25]. Briefly, 1.35 mmol, 0.3 mmol, and 0.7 mmol of $\text{Fe}(\text{acac})_3$, ZnCl_2 , and FeCl_2 , respectively, were mixed into a round bottom flask with 20 mL of tri-*n*-octylamine, 6 mmol of both oleic acid and oleylamine, and 10 mmol of 1,2 hexadecanediol. The reaction mixture was then heated up to 200°C for 2 h. From here, the mixture was heated to 305°C for 2 h and the nanoparticles were purified by repeatedly washing with ethanol.

To coat the MNP cores with a mSi shell, a modified procedure from what was reported by Hyeon et al. was used [26]. 5 mg of the

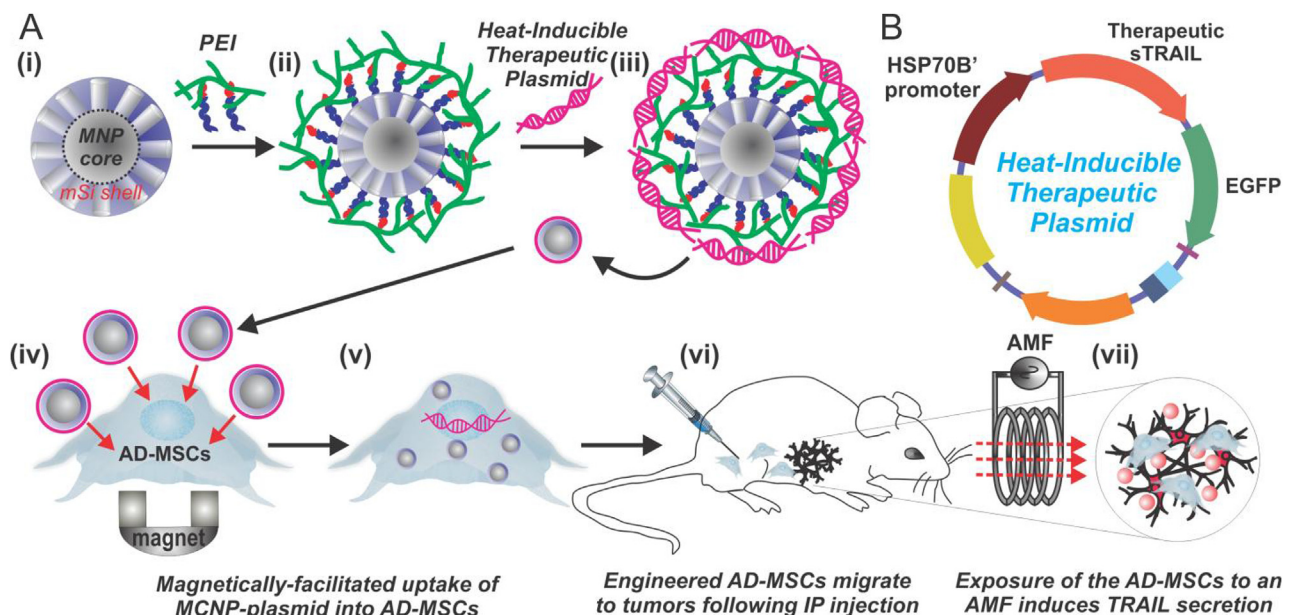


Fig. 1. Mild Magnetic Hyperthermia-Activated Stem Cell-Based Gene Therapy. A) MCNPs composed of a ZnFe_2O_4 magnetic nanoparticle (MNP) core and a mesoporous silica (mSi) shell (i) are functionalized with polyethyleneimine (PEI) to allow for complexing with a heat-inducible therapeutic plasmid (ii–iii). The MCNPs enhance delivery of the heat-inducible plasmid into the adipose-derived mesenchymal stem cells (AD-MSCs) via magnetically-facilitated uptake (iv–v). These engineered AD-MSCs can then be injected *in vivo* (vi), where they innately home to the tumors/metastases. Finally, mild magnetic hyperthermia, via exposure of the MCNPs to an alternating magnetic field (AMF), can be used to specifically activate the heat-inducible secretion of therapeutic TRAIL from the AD-MSCs (vii). B) The heat-inducible plasmid is composed of a HSP70B' promoter and a secreted form of TRAIL (sTRAIL) that is fused to an EGFP reporter.

alkyl-capped MNP cores dispersed in chloroform were sonicated using a probe type sonicator in a 0.1 M aqueous cetyltrimethylammonium bromide (CTAB) solution. Upon evaporation of chloroform, the CTAB capped MNP cores were diluted to 50 mL with water and the pH of this mixture was adjusted to ~11 using a 2M NaOH solution. This reaction mixture was heated to 70 °C and, under vigorous stirring, 0.4 mL of tetraethylorthosilicate (TEOS) in 2.4 mL of ethyl acetate was added. After the addition of TEOS, the reaction was allowed to continue for 4 h. The MCNPs were collected and washed several times with ethanol. To remove the template, the nanoparticles were heated to 60 °C in an ammonium nitrate solution. The extracted MCNPs were again washed with ethanol. Finally, the MCNPs were characterized by high-resolution Transmission electron microscopy (HR-TEM) and Fourier-transform infrared spectra (FTIR).

To characterize the magnetic properties of the nanoparticles, the resulting MCNPs (25 µg/mL in H₂O) were exposed to an AMF (5 kA/m, 225 kHz) using a solid-state induction heating system (Superior Induction Company) for 1 h. The temperature of the solution was monitored using a fiber optic temperature probe (LumaSense Technologies). To calculate the specific absorption rate (SAR), the following equation was used:

$$SAR (W/g) = C \left(\frac{dT}{dt} \right) \left(\frac{m_s}{m_m} \right)$$

where C is the specific heat capacity, m_s is the mass of the solution, m_m is the mass of the magnetic nanoparticles, T is the temperature, and t is the time [27].

2.2. Construction of the plasmids

To construct the plasmids, we first cloned the recombinant gene that encodes a secreted form of the human TRAIL protein into the pEGFP-N1 backbone (Clontech) thereby creating a secretable TRAIL-EGFP fusion that is constitutively active (e.g. via CMV promoter) to allow for monitoring (sTRAIL-EGFP plasmid). In particular, the secreted form of TRAIL was kindly provided by Drs. Leaf Huang (Department of Biomedical Engineering, University of North Carolina at Chapel Hill) and Yukai He (Cancer Center, Georgia Health Sciences University) [28]. This recombinant TRAIL gene (sTRAIL) was composed of the soluble form of the human Flt3L gene (hFlex) at the 5' end and the human TRAIL gene at the 3' end (aa residues 95–281) with an isoleucine zipper at the N-terminal of TRAIL, which was previously shown to significantly enhance trimerization of the fusion protein as well as its anti-tumor activity [28]. As such, the cDNA for sTRAIL was amplified using PCR by employing the 5' and 3' primers 5'-CGGCCGCTCGAGATGACAGTGCTGGCGCA-3' and 5'-CGCCGCAAGCTTTAGCCAACTAA AAAGGC-3', respectively. In this way, the 5' end of the PCR product contained the XhoI restriction site and the 3' end of the PCR product contained the HindIII site. This 1 kb PCR product was digested with XhoI/HindIII and then cloned into pEGFP-N1 to create the sTRAIL-EGFP fusion. The plasmid was denoted sTRAIL-EGFP. Similarly, HSP70B' was ordered from Addgene (Plasmid #19486) [29]. The cDNA for the HSP70B' promoter was amplified using PCR by employing the 5' and 3' primers 5'-GACAATTAATACCATGCAGGCCACGGGAGCT-3' and 5'-CGGCGCTCGAGTCAATCAACCTCTCAATGA-3', respectively. In this way, the 5' end of the PCR product contained the AseI restriction site and the 3' end of the PCR product contained the XhoI site. This 200 bp PCR product was digested with AseI/XhoI and then cloned into the sTRAIL-EGFP plasmid thereby creating the final HSP-sTRAIL plasmid. The open reading frames of the fusion proteins were confirmed by DNA sequencing (Macrogen).

2.3. Formation of MCNP-PEI/plasmid complexes

To prepare the aforementioned MCNPs for plasmid delivery, the negatively charged MCNPs were coated with a branched cationic polymer, polyethyleneimine (PEI), which affords the MNPs with an overall positive charge. PEI is a polymer that is partially protonated under physiological conditions, thus allowing for the formation of complexes in the presence of nucleic acids [30]. PEIs have been used extensively for the delivery of plasmids and nucleic acids including small interfering RNAs (siRNAs) and microRNAs [30–32]. Specifically, it has been demonstrated that PEI-based complexes are able to enter the cell via caveolae- or clathrin-dependent routes and are able to facilitate release from the endosome with high efficiency via the “proton sponge effect [33].”

To obtain PEI-coated MCNPs, the MCNPs, dispersed in a minimal amount of ethanol, were added to a stirring solution containing excess PEI (MW = 25,000; Mn = 10,000) and 20 mM NaCl. This PEI molecular weight (MW) and structure was chosen based on previous reports [34]. After spinning overnight, the PEI-coated MCNPs were filtered using a centrifugal filter unit (EMD Millipore, 10,000 MW) to remove excess PEI. To complex the PEI coated MCNPs with plasmid, MCNP-PEI was diluted in a 20 mM NaCl solution and plasmid was added to the solution. Complexing was allowed to occur for 20 min.

To determine the initial concentration of MNP-PEI that needed to be added to complex 200 ng/mL of plasmid, complexes with increasing concentrations of MNP-PEI were incubated with 200 ng/mL of plasmid. Afterwards, 100 µL of solution were transferred to a 96-well (black-walled, clear-bottom, non-adsorbing) plate (Corning, NY, USA). A total of 100 µL of diluted PicoGreen dye (1:200 dilution in Tris–EDTA (TE) buffer) was added to each sample. Fluorescence measurements were made after 10 min of incubation at room temperature using a M200 Pro Multimode Detector (Tecan USA Inc, NC, USA), at an excitation and emission wavelength of 480 and 520 nm, respectively. All measurements were corrected for background fluorescence from a solution containing only buffer and PicoGreen dye.

To characterize the MCNP-PEI/plasmid complexes, dynamic light scattering (DLS) and Zeta Potential analyses were performed using a Malvern Instruments Zetasizer Nano ZS-90 instrument (Southboro, MA) with reproducibility being verified by the collection and comparison of sequentially obtained measurements. MCNP-PEI/plasmid complexes, were prepared using purified water (resistivity = 18.5 MΩ-cm). DLS measurements were performed at a 90° scattering angle at 25 °C. Z-average sizes of three sequential measurements were collected and analyzed. Zeta potential measurements were collected at 25 °C, and the Z-average potentials following three sequential measurements were collected and analyzed.

2.4. Transfecting cells with MCNP-PEI/plasmid complexes

Twenty-four hours before the magnetofection of MCNP complexes, A2780 ovarian cancer (ATCC) or human adipose-derived mesenchymal stem cells (AD-MSCs from Lonza [catalog # PT-5006]) were seeded into each well of a 12-well plate, so as to attain 80% confluency at the time of transfection. MNP-PEI/plasmid complexes were formed as described above. Thereafter, the MCNP complexes were mixed with Opti MEM (Life Technologies) and added to each well to attain the desired final concentration of plasmid/well. Subsequently, the cell culture plates were placed on a static Nd-Fe-B magnetic plate (OZ Biosciences, France) for 10 min (as optimized from previous reports) [23]. The culture plates were placed back into the incubator for 5 h and afterwards, the cells were washed with DPBS and the transfection medium was replaced with

fresh growth medium. The growth mediums for the cell lines (obtained from ATCC or Lonza) used in the study are as follows: A2780 (DMEM supplemented with 10% FBS, 1% Penicillin-Streptomycin, and 1% Glutamax) and AD-MSCs (Lonza ADSC Basal Medium [Catalog # PT-3273] with ADSC-GM SQ kit [Catalog # PT-4503]).

2.5. Magnetic hyperthermia

Twenty-four hours after transfection, cells were washed with DPBS, trypsinized, and exposed to an AMF (5 kA/m, 225 kHz) for the desired amount of time. In particular, to achieve a constant temperature of -41°C , the cells were initially exposed to an AMF for 20 min to achieve a temperature of -43°C . Afterwards, the cells were periodically exposed to the AMF (5 min on, 5 min off) to maintain the temperature at -41°C . Thereafter, fresh media was added to the treated cells and the cells were plated back into 12-well plates.

2.6. Cell viability assays

The percentage of viable cells was determined by MTT assay following standard protocols as described by the manufacturer. All measurements were made 48 h after initial transfection. All experiments were conducted in triplicate and averaged. The data is represented as formazan absorbance at 490 nm, considering the control (untreated) cells as 100% viable.

2.7. Mild magnetic hyperthermia-activated TRAIL expression from AD-MSCs to induce apoptosis in ovarian cancer cells

24 h after the transfection of AD-MSCs with MCNP-PEI/plasmid complexes (50 $\mu\text{g}/\text{mL}$ MCNP, 200 ng/mL of plasmid), we exposed the cells to an AMF (same conditions as described previously) to maintain a temperature of approximately 41°C for 1 h. About 72 h after initial transfection, we collected the conditioned media from the engineered AD-MSCs, which contain TRAIL that was secreted from the engineered AD-MSCs, and added it (60:40 ratio with normal A2780 growth media) to the A2780 ovarian cancer cells. Following an additional incubation of 48 h, its therapeutic efficacy was evaluated using MTT assay.

2.8. Cell differentiation

To confirm the osteogenic potential of the MSCs used, AD-MSCs were incubated in CEM until a confluent layer was achieved and then osteogenic medium was added, containing IMDM supplemented with 9% FBS, 9% HS, 2 mM L-glutamine, 100 U/mL penicillin, 100 $\mu\text{g}/\text{mL}$ streptomycin, 50 ng/mL L-thyroxine (Sigma Aldrich), 20 mM β -glycerol phosphate, (Sigma Aldrich), 100 nM dexamethasone (Sigma Aldrich) and 50 μM ascorbic acid (Sigma Aldrich). Medium was changed every 3–4 days. After 21 days, cells were fixed in 10% formalin, rinsed with DPBS and Alizarin Red S assay was used to assess mature bone differentiation. In particular, DPBS was removed and the Alizarin Red solution (40 mM, pH 4.2) was added to each well and kept for 30 min with gentle shaking. The pH of the Alizarin Red solution was carefully adjusted using a pH meter (Accumet Basic, AB15, Fisher Scientific, USA). The solution was then removed and cells were washed with DI water five times. Following, the calcium-stained cells were imaged using an optical microscope (Eclipse Ti-U, Nikon, Japan). To quantitative these results, cells were destained using 10% cetylpyridinium chloride (CPC) in 10 mM sodiumphosphate (pH 7.0) for 30 min at room temperature. Finally, the concentration Alizarin Red S was determined by measuring its absorbance at 562 nm on a multiplate reader (Tecan, Switzerland).

2.9. Immunocytochemistry

Cell cultures were fixed with 4% formaldehyde (Thermo-Scientific) for 15 min, blocked for 1 h with 5% normal goat serum (NGS, Life Technologies), and permeabilized with 0.3% Triton X-100 when staining for intracellular markers (Ki-67). The primary antibody for Ki-67 (1:400, Cell Signaling, catalog # 9449S) was incubated overnight at 4°C . Alexa Fluor 546-conjugated secondary antibodies were used to detect the primary antibodies (1:200, Molecular Probes) and Hoechst 33342 (1:100, Life Technologies) was used as a nuclear counterstain. The substrates were mounted on glass slides using ProLong[®] Gold antifade (Life Technologies) and imaged using a Nikon TE2000 Fluorescence Microscope.

2.10. PCR analysis

Total RNA was extracted 48 h after initial transfection using Trizol Reagent (Life Technologies) and the mRNA expression level of genes of interest (Table S1) were analyzed using quantitative PCR (qPCR). Specifically, cDNA was generated from 1 μg of total RNA using the Superscript III First-Strand Synthesis System (Life Technologies). Analysis of the mRNA was then accomplished using primers specific to each of the target mRNAs. qPCR reactions were performed using SYBR Green PCR Master Mix (Applied Biosystems) on a StepOnePlus Real-Time PCR System (Applied Biosystems) and the resulting Ct values were normalized to GAPDH. Standard cycling conditions were used for all reactions with a melting temperature of 60°C . Primers are listed in Table S1.

2.11. Mechanistic studies

For the blocking experiments, A2780 ovarian cancer cells were incubated in growth medium containing 10 $\mu\text{g}/\text{mL}$ of the respective blocking antibodies for 1 h before the addition of conditioned media from the engineered AD-MSCs (60:40 ratio with normal A2780 growth media). In particular, mouse monoclonal TRAIL-R1/DR4 (Enzo Life Sciences) and mouse monoclonal TRAIL-R2/DR5 (Enzo Life Sciences) antibodies were used for these experiments. Cell viability was then evaluated 24 h after the addition of conditioned media using MTT assay.

To inhibit caspases, the pan-caspase inhibitor, Z-VAD-FMK (Enzo Life Sciences), and the caspase-8 inhibitor, Z-IETD-FMK (Enzo Life Sciences), were used. For Z-VAD-FMK, a 10 mM stock solution of the inhibitor was prepared using DMSO and the final concentration of the inhibitor and DMSO that the A2780 ovarian cancer cells were exposed to was 20 μM and 0.1%, respectively. For Z-IETD-FMK, a 10 mM stock solution of the inhibitor was prepared using DMSO and the final concentration of the inhibitor and DMSO that the A2780 ovarian cancer cells were exposed to was 2 μM and 0.1%, respectively. The A2780 ovarian cancer cells were treated with the inhibitors at the same time as the addition of the conditioned media (60:40 ratio with normal A2780 growth media). Cell viability was then evaluated 24 h after the addition of conditioned media and inhibitors using MTT assay.

For TRAIL immunoprecipitation, MCNPs were conjugated with TRAIL monoclonal antibodies (Santa Cruz Biotechnology). For this purpose, the MCNPs were first functionalized with primary amines via the grafting of aminopropyltriethoxysilane (APTES). This was performed by refluxing up to 50 mg of MCNPs in 40 mL of toluene with 20 μL of APTES overnight under dry conditions. The resulting amine-functionalized MCNPs were then washed several times with ethanol and resuspended in DMF. The TRAIL antibody (30 μL of 0.1 mg/mL solution) was activated with EDC/NHS coupling in 250 μL of DMF. Then, 1 mg of MCNPs dispersed in 250 μL of DMF was added to the activated TRAIL antibody and allowed to stir

overnight. The resulting particles were washed several times with water and finally resuspended in DPBS. To perform MCNP-based immunoprecipitations, 200 μL of the antibody-conjugated MCNPs (1 mg/mL) was added to 500 μL of conditioned media and incubated on ice for 30 min. To separate the nanoparticles from the conditioned media, a magnet was placed on the side of the tube for 5 min and the supernatant was carefully collected and transferred to a new tube. The supernatant was then added to A2780 cells (60:40 ratio with normal A2780 growth media) and cell viability was evaluated 24 h later using MTT assay.

2.12. Animal studies

Human ovarian cancer cells (A2780) expressing the luciferase enzymes were purchased from Cell Biolabs, Inc (San Diego, CA). Cells were cultured in DMEM media with L-glutamine (Lonza, Walkersville, MD) supplemented with 10% fetal bovine serum (Invitrogen, Carlsbad, CA), and 1.2 mL/100 mL penicillin-streptomycin (Gibco, Grand Island, NY). All cells were grown in a humidified atmosphere of 5% CO_2 (v/v) at 37 °C. All experiments were performed on the cells in the exponential growth phase.

6–8 weeks old Athymic nu/nu mice (NCRNU-M, CrTac: NCr-Foxn1nu) were obtained from Taconic (Hudson, NY, USA). All mice were maintained in micro-isolated cages under pathogen free conditions in the animal maintenance facilities of Rutgers, The State University of New Jersey. The research involving animals has been reviewed and approved by the Institutional Animal Care and Use Committee before any research was conducted. Orthotopic (intra-peritoneal) ovarian cancer model was created by intraperitoneally injecting 2×10^6 ovarian cancer cells (A2780) labeled with luciferase into the mice. Luciferase transfected cancer cells were visualized in live anesthetized animals using an *in vivo* bioluminescence IVIS system (Xenogen, Alameda, CA). Luciferin (150 mg/kg) was intraperitoneally administered 10 min before imaging. Mice were anesthetized with isoflurane (4% for induction of anesthesia and 1–2% for maintenance) using a XGI-8 Gas Anesthesia System (Xenogen, Alameda, CA) for imaging as previously described [35,36].

After allowing up to 2 weeks for the tumors to develop, AD-MSCs were administered. For AD-MSC injection, AD-MSCs were engineered with MCNP-PEI/plasmid complexes as described above. 24 h after transfection, Vybrant DiD Cell-labeling solution was used (Molecular Probes, Catalog # V-22887) to label the cells prior to administration to animals. Specifically, staining media was prepared by adding 5 μL of the supplied DiD solution for every 1 mL of normal growth media required. The media from the engineered or unengineered AD-MSCs were then removed and replaced with staining media. AD-MSCs were incubated with staining media for 30 min. Afterwards, the labeled AD-MSCs were washed three times with DPBS, trypsinized, and then resuspended such that there were 5×10^5 cells per 300 μL DPBS. As such, each animal received an intraperitoneal injection of 5×10^5 cells in 300 μL of DPBS. As a control, a single dose of 200 μL (5 mg/kg) of recombinant TRAIL (ProSpec) in DPBS was injected intraperitoneally on day 0. Tumor volume of all animals was then monitored over two weeks by monitoring tumor luminescence. Please note that each group in each experiment had at least three mice.

3. Results and discussion

3.1. Synthesis and characterization of the magnetic core-shell nanoparticles

For the dual purpose of delivering a heat-inducible therapeutic plasmid to the stem cells as well as spatiotemporally activating the

plasmid via mild magnetic hyperthermia, we synthesized MCNPs with a zinc-doped iron oxide (ZnFe_2O_4) core. These cores have previously been shown to have a significantly higher saturation magnetization when compared to conventional Fe_2O_3 or Fe_3O_4 magnetic nanoparticles (MNPs) [25]. As such, we first synthesized ZnFe_2O_4 cores with a doping percentage of $(\text{Zn}_{0.4}\text{Fe}_{0.6})\text{Fe}_2\text{O}_4$ via the thermal decomposition of a mixture of metal precursors (zinc chloride, ferrous chloride, and ferric acetylacetonate) in the presence of oleic acid and oleylamine using a previously reported protocol that was modified by our group [23,25]. Following core synthesis, an inert mSi shell was formed via the condensation of TEOS in the presence of a CTAB micelle template [26]. TEM revealed that the diameter of the cores was 18.93 ± 1.6 nm and that the MNP cores were uniformly coated with a 33.91 ± 3.8 nm thick mSi shell. As a result, the overall diameter of the as-synthesized MCNPs was 88.03 ± 8.22 nm (Fig. 2A). For more detailed characterization, HR-TEM revealed the monocrystalline structure of the MNP cores with a lattice fringe that was measured to be 4.8 Å (Fig. S1A), which is characteristic of the (111) plane of the spinel [23,25]. Finally, FTIR analysis was used to confirm that the CTAB template had been extracted and removed from the pores of the mSi shell (Fig. S1B). In addition, the pores were estimated to be approximately 3 nm in diameter based on HR-TEM (Fig. 2B) as well as previous reports [26].

To prepare the aforementioned MCNPs for plasmid delivery, the MCNPs were coated with branched polyethylenimine (PEI, MW = 10 kDa) via electrostatic interactions in the presence of NaCl to afford the MCNPs with an overall positive charge. As a result, this would facilitate MCNP complexation with negatively-charged plasmid DNA and induce endosomolysis within the cytoplasm [37]. To minimize cytotoxicity while maximizing transfection efficiency, we used 10 kDa branched PEI, which has previously been demonstrated to be biocompatible with stem cells [21,38]. The resulting water soluble PEI-coated MCNPs (MCNP-PEI) had a hydrodynamic size of 117.2 ± 37 nm (polydispersity index [PDI] = 0.177) as measured by dynamic light scattering (DLS) and a zeta potential of $+44.23 \pm 0.72$ mV (Fig. 2C and S2A).

Finally, the MCNPs were characterized by a specific absorption rate (SAR) of 564 W/g, which was determined using an AMF with amplitude of 5 kA/m and a frequency of 225 kHz. This SAR is consistent with data reported in the literature for similar ZnFe_2O_4 MNPs [21,39]. Moreover, we demonstrated that these MCNPs (25 $\mu\text{g}/\text{mL}$) could reach temperatures as high as 47 °C within an hour of exposure to the AMF (Fig. 2D) and that we could maintain a mild hyperthermia temperature of 41–43 °C following periodic exposure to the AMF (5 min on, 5 min off, Fig. S2B). As such, we were able to synthesize monodisperse water-soluble MCNPs with a narrow size distribution and, more importantly, these MCNPs had excellent magnetic properties for magnetic hyperthermia even after the addition of an mSi shell.

3.2. Heat-inducible plasmid construction

Next, in order to attain control over the secretion of TRAIL from the engineered stem cells using mild magnetic hyperthermia, we constructed a heat-inducible TRAIL plasmid using the HSP70B' promoter (HSP-sTRAIL plasmid, Fig. 3A). To this end, we first cloned the recombinant gene that encodes a secreted form of the human TRAIL protein into the pEGFNP-N1 backbone (Clontech), thereby creating a secretable TRAIL-EGFP fusion that was constitutively active due to its CMV promoter (sTRAIL-EGFP plasmid, Fig. 3A(i)). Specifically, this recombinant TRAIL gene was composed of the soluble form of the human Flt3L gene (hFlex) at its 5' end and the human TRAIL gene at its 3' end with an isoleucine zipper at the N-terminal of TRAIL, which was previously shown to significantly

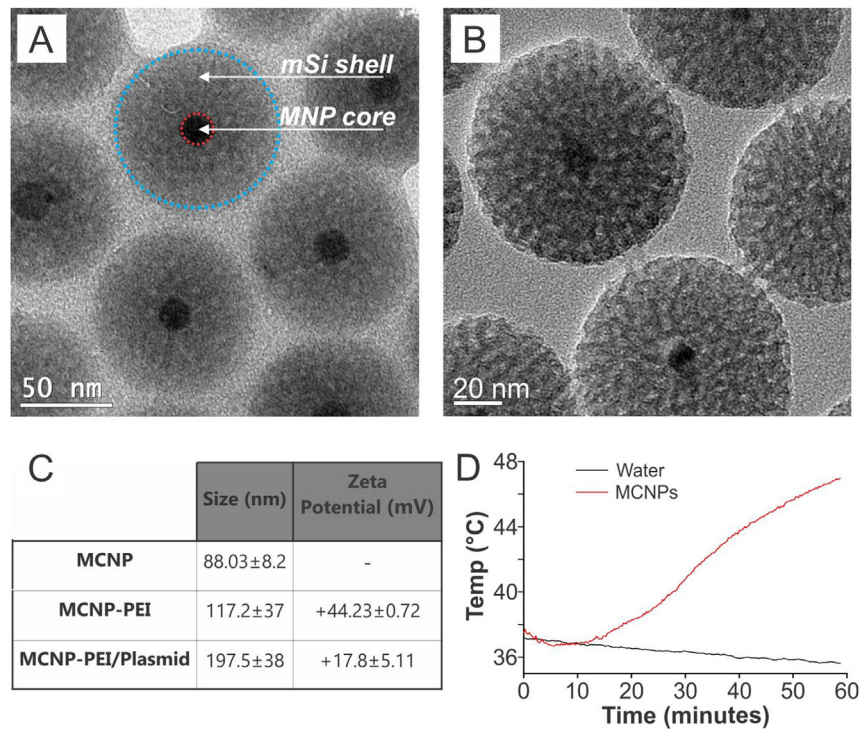


Fig. 2. Characterization of the MCNPs. A) HR-TEM image of the MCNPs. B) Higher magnification HR-TEM image of the MCNPs shows that the pores are about 3 nm in size. C) Size was determined using TEM and dynamic light scattering (DLS). Moreover, the Zeta potential was confirmed. The values in the chart are given as mean \pm standard deviation. D) The MCNPs (25 μ g/mL) can be heated to temperatures as high as 47 $^{\circ}$ C after exposure to an alternating magnetic field (5 kA/m, 225 kHz) for 1 h.

enhance the trimerization of the fusion protein as well as its anti-tumor activity [28]. Following insertion of the recombinant TRAIL gene into pEGFP-N1, the CMV promoter of the resultant sTRAIL-EGFP plasmid was replaced with a HSP70B' promoter (Fig. 3A(ii)) to enable strict remote control of gene expression using MCNP-mediated mild magnetic hyperthermia, thereby forming the final HSP-sTRAIL plasmid construct. In particular, the human HSP70B' promoter has previously been shown to exhibit highly specific heat inducibility with low background activity when compared to other heat shock promoters (e.g. HSP70) [40,41], which can be activated by a number of stresses besides heat (e.g. heavy metal-induced oxidative stress) [20]. To confirm the successful construction of the plasmid, all steps were evaluated via restriction enzyme analysis (Fig. S3) and DNA sequencing.

Following plasmid construction, we determined whether the recombinant plasmids could produce the TRAIL protein. For this purpose, we performed a simple proof-of-concept study by delivering the constitutively active sTRAIL-EGFP plasmid into A2780 ovarian cancer cells. About 48 h after initial transfection, total RNA was collected and reverse transcription PCR (RT-PCR) was performed (Fig. 3B). From these results, we confirmed that TRAIL is produced, whereas it is not present in control samples, which consisted of cells that had been transfected with an EGFP plasmid. Lastly, we confirmed that heat could be used to specifically induce TRAIL expression in cells transfected with the HSP-sTRAIL plasmid. For this purpose, 24 h after initial transfection, the cells were subjected to mild hyperthermia (41 $^{\circ}$ C) for 1 h via exposure to a water bath. Then, 48 h after initial transfection, fluorescence microscopy images of the cells transfected with the heat-inducible HSP-sTRAIL plasmid with and without exposure to mild hyperthermia were taken to visualize the expression of the TRAIL-EGFP fusion (Fig. 3C). These images clearly demonstrate that engineered cells only express EGFP when exposed to mild hyperthermia. As confirmation, RNA was also collected from samples with

and without exposure to mild hyperthermia. qPCR analysis of these samples demonstrated that following mild hyperthermia at 41 $^{\circ}$ C for 1 h, TRAIL expression was significantly increased (3-fold, $p < 0.05$) compared to samples that were not exposed to mild hyperthermia (Fig. 3D). Altogether, these results confirm that the constructed HSP-sTRAIL plasmid can induce the expression of TRAIL in a heat-specific manner.

3.3. Engineering MSCs with the MCNP-PEI/Plasmid complexes

Following plasmid construction and initial proof-of-concept studies, we sought to optimize the MCNP-based transfection into stem cells. For this purpose, we engineered adipose-derived MSCs (AD-MSCs) with our MCNP-PEI/plasmid complexes as AD-MSCs represent an abundant and accessible source of adult stem cells with the ability to differentiate into multiple lineages [42]. Before engineering the AD-MSCs, we initially transfected the AD-MSCs with MCNP-PEI alone to determine the optimal concentration of MCNP-PEI that can be delivered while minimizing cytotoxicity. We observed that the delivery of MCNP-PEI alone had minimal cytotoxicity even at concentration as high as 100 μ g/mL (~85% cell viability 48 h after transfection, Fig. S4A). As such, we used 50 μ g/mL for future steps as this concentration induced almost no cytotoxicity (~95% cell viability) while also exhibiting robust heating capabilities. Next, to complex the PEI-coated MCNPs with the HSP-sTRAIL plasmid, we mixed the two components together and incubated them at room temperature for 20 min. Final characterization of these MCNP-PEI/plasmid complexes demonstrated that the size of the MCNP-PEI/plasmid complexes, as measured by DLS, increased to a final diameter of 197.5 \pm 38 nm (PDI = 0.410) and retained a positive zeta potential of +17.8 \pm 5.11 mV (Fig. 2C).

Subsequently, to engineer the AD-MSCs with our MCNP-PEI/plasmid complexes, we delivered MCNP-PEI/plasmid complexes wherein 50 μ g/mL of MCNP were complexed with increasing

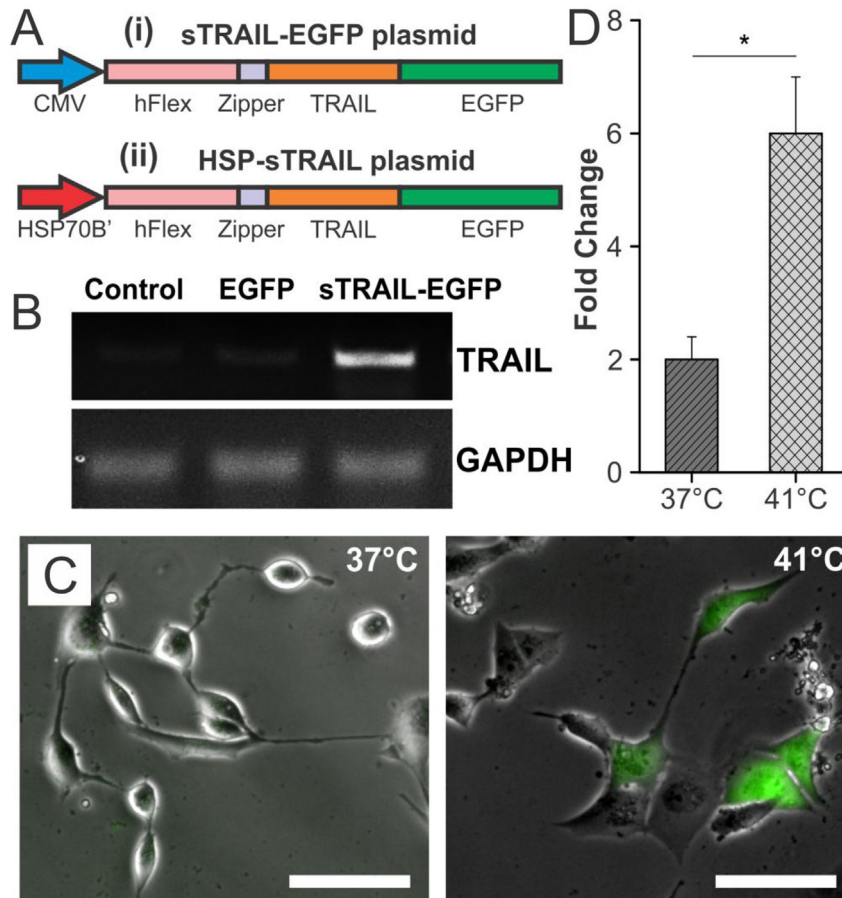


Fig. 3. Characterization of the Heat-Inducible Plasmid. A) Schematic depicting the sTRAIL-EGFP plasmid (i), which expresses a sTRAIL-EGFP fusion that is constitutively active, and the HSP-sTRAIL plasmid (ii), which expresses the same sTRAIL-EGFP fusion under the control of a heat-inducible HSP70B' promoter. B) RT-PCR demonstrating the successful synthesis of the sTRAIL-EGFP plasmid, which was transfected into A2780 ovarian cancer cells. C) Proof-of-concept demonstrating that the HSP-sTRAIL plasmid can be specifically activated by heat (1 h at 41 °C in a water bath) as seen via fluorescence imaging due to fusion of TRAIL with EGFP. Scale bar = 50 μ m. D) Confirmation of heat-specific TRAIL activation was obtained using qPCR (* $p < 0.05$) and was normalized to transfected cells that were incubated at 37 °C. GAPDH was used as the housekeeping gene.

concentrations of HSP-sTRAIL plasmid to determine the maximal amount of plasmid that could be delivered with our MCNPs without significantly affecting AD-MSC viability. From this optimization process, we determined that a plasmid concentration of 200 ng/mL was optimal. Moreover, it was found that this amount of plasmid could be completely complexed using 50 μ g/mL of MCNP as determined via Picogreen assay, which is a dye that binds to free double-stranded DNA (Fig. S4B). Using the optimized complexing and transfection conditions, the AD-MSCs maintained a cell viability of ~90% following the engineering process (Fig. S4C). To characterize the affect that engineering had on AD-MSC proliferation in more detail, we performed immunocytochemistry for Ki-67 (Fig. 4A), which is a mitotic marker that is expressed during all phases of the cell cycle except during G₀. It was observed that approximately 20% of the AD-MSCs expressed Ki-67 and that there was no statistically significant difference between the number of Ki-67 expressing engineered AD-MSCs and unengineered AD-MSC controls (Fig. 4B).

3.4. Characterizing the engineered AD-MSCs

After engineering the AD-MSCs with MCNP-PEI/plasmid complexes, we next sought to determine whether the act of engineering the AD-MSCs negatively affected their ability to differentiate and, more importantly, to migrate to cancers *in vivo*. AD-MSCs are multipotent cells that have been shown to readily differentiate

along osteogenic, chondrogenic, and adipogenic lineages. Therefore, to confirm that the process of engineering did not compromise the ability of the AD-MSCs to differentiate, we compared the ability of engineered and unengineered control AD-MSCs to differentiate along an osteogenic lineage. Briefly, to induce differentiation along this lineage, the engineered or unengineered AD-MSCs were exposed to osteogenic differentiation media for three weeks (Fig. S5) [43]. After this differentiation period, osteogenic differentiation was quantified via Alizarin Red S (ARS) staining, which is typically used to evaluate calcium deposited by cells in culture, and qPCR. ARS staining revealed calcium-rich deposits in both engineered and unengineered osteogenic AD-MSCs (Fig. 5A). Quantification suggested that the osteogenic differentiation capability was unaffected by the act of engineering as there was no statistically significant difference between the quantity of calcium deposited by engineered AD-MSCs and unengineered AD-MSC controls (Fig. 5B). Further confirming these results, we performed qPCR on key osteogenic genes including osteonectin (ON), bone alkaline phosphate (BAP), osteocalcin (OCN), and osteopontin (OPN). As expected, all four genes were highly expressed when normalized to non-differentiated control AD-MSCs (Fig. 5C) and no significant difference was found between the engineered osteogenic AD-MSCs and the unengineered osteogenic AD-MSCs.

Next, we confirmed that the act of engineering the AD-MSCs did not negatively affect their ability to migrate to ovarian tumors *in vivo* (Fig. 5D). To this end, we established a metastatic model of

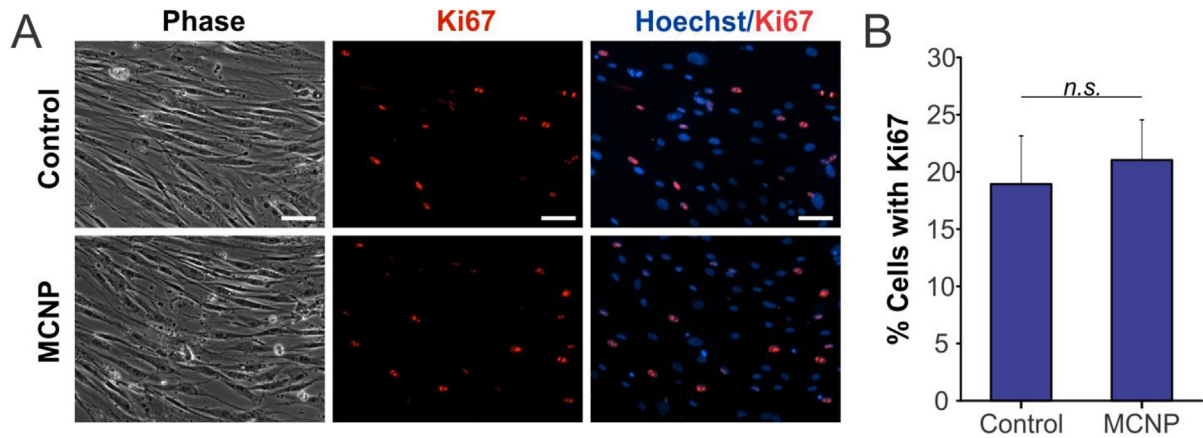


Fig. 4. Proliferation of AD-MSCs Engineered with MCNP-PEI/Plasmid Complexes. A) The proliferation of unengineered (control) and engineered (MCNP-PEI/plasmid) AD-MSCs was evaluated using Ki-67 (red). The nuclei were stained with Hoechst (blue). Scale bar = 50 μ m. B) Approximately 20% of the AD-MSCs expressed Ki-67 and there was no statistically significant difference between the two groups ($p > 0.05$). (For interpretation of the references to colour in this figure legend, the reader is referred to the web version of this article.)

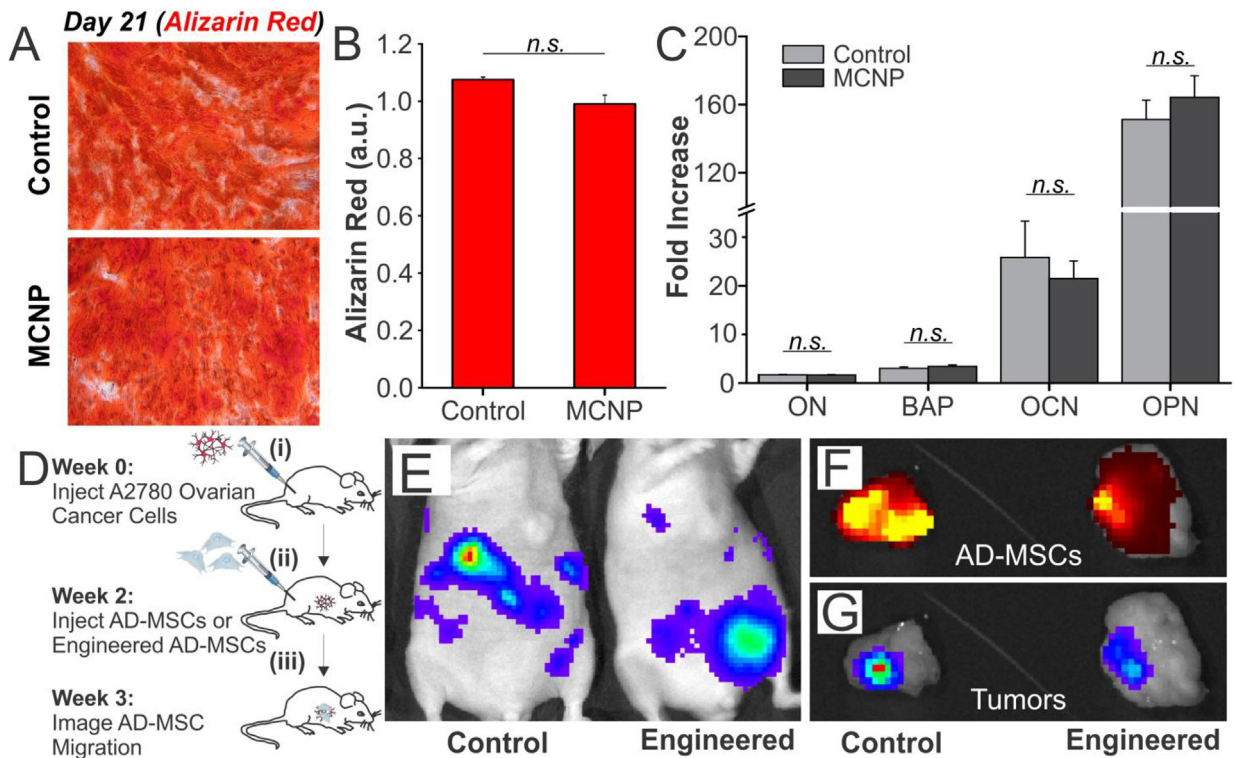


Fig. 5. Differentiation and Migration of AD-MSCs Engineered with MCNP-PEI/plasmid Complexes. A) To evaluate osteogenic differentiation, engineered or unengineered AD-MSCs were differentiated for three weeks. Osteogenesis was then quantified via Alizarin Red staining. B) Quantification of staining suggested that there was no statistically significant difference between the two groups ($p > 0.05$). C) qPCR of key osteogenic genes demonstrated that all four genes were highly expressed over non-differentiated control and that no significant difference was found between the engineered and unengineered AD-MSCs ($p > 0.05$). GAPDH was used as the housekeeping gene. D) Timeline of the studies used to evaluate the tumor homing ability of the engineered and unengineered AD-MSCs. E) Luciferase was used to identify the A2780 cells. Luminescence imaging shows the establishment of disseminated A2780 tumors. The luminescence intensity goes from blue to red, wherein blue is the weakest and red is the strongest. F) One week after the injection of AD-MSCs, tumors were collected. Fluorescence imaging shows the DiD-labeled engineered and unengineered AD-MSCs. The fluorescence intensity goes from dark red to yellow, wherein dark red is the weakest and yellow is the strongest. G) Luminescence imaging of the conglomerated tumors demonstrates that the AD-MSCs are able to colocalize with the tumors. (For interpretation of the references to colour in this figure legend, the reader is referred to the web version of this article.)

ovarian cancer wherein two million A2780 ovarian cancer cells were injected intraperitoneally (i.p.) into female nude mice (Fig. 5D(i)). To confirm that the engineered AD-MSCs could colocalize with ovarian tumors, the mice, which had disseminated peritoneal A2780 tumors, were injected with half a million engineered AD-MSCs or unengineered AD-MSC controls i.p. at 7 days post-tumor implantation (Fig. 5D(ii)). Mice were then harvested

after an additional 7 days (Fig. 5D(iii)). Multimodality imaging was used to identify the various components; luciferase was used to identify the A2780 ovarian cancer cells (Fig. 5E) and a lipophilic DiD dye was used to label the engineered and unengineered AD-MSCs. From Fig. 5F and G, it can be observed that, after the tumors were collected (week 3), the DiD-labeled engineered AD-MSCs (Fig. 5F) co-localized with the luciferase labeled A2780 cells (Fig. 5G) within

one week of AD-MSC injection (Figs. S6 and S7). Importantly, it can be seen that there was no significant difference between the colocalization of engineered AD-MSCs and unengineered AD-MSC controls. As such, these results suggest that the engineered AD-MSCs can act as an effective delivery vehicle for gene therapy.

3.5. Mild magnetic hyperthermia-activated TRAIL expression from AD-MSCs can effectively induce apoptosis in ovarian cancer cells

TRAIL-expressing MSCs have previously been shown to have the ability to induce cancer cell death and decrease tumor and metastasis development *in vivo* [14]. In these experiments, the TRAIL expression was either constitutively active or conditionally activated with the addition of doxycycline. However, while TRAIL is largely biocompatible with normal cells, as mentioned previously, there have been reports demonstrating potential hepatotoxicity in preclinical models when treated with recombinant TRAIL [18,19].

Addressing this major limitation, we engineered AD-MSCs with MCNP-PEI/plasmid complexes, where the plasmid was the heat-inducible HSP-sTRAIL, in order to gain spatiotemporal control over therapeutic gene expression. Having already determined that mild hyperthermia (induced using a water bath) could be used to activate this plasmid, we next sought to induce TRAIL expression from the engineered AD-MSCs using mild magnetic hyperthermia, which can be induced remotely and non-invasively by exposing the engineered AD-MSCs to an AMF. To this end, we employed the experimental design illustrated in Fig. 6A. In particular, 24 h after transfection of the AD-MSCs with MCNP-PEI/plasmid complexes, we exposed the cells to an AMF (same conditions as described previously) to maintain a temperature of approximately 41 °C for 1 h (Fig. 6B and S2B). About 72 h after initial transfection, we collected the conditioned media from the engineered AD-MSCs, which contain TRAIL that was secreted from the engineered AD-MSCs, and added it (60:40 ratio with normal A2780 growth media) to the A2780 ovarian cancer cells. Following an additional incubation of 48 h, its therapeutic efficacy was evaluated. Importantly, our first observation was that mild magnetic hyperthermia alone did not significantly affect AD-MSC viability, which agrees with previously published results on the effects of heat on stem cell viability (Fig. 6C) [44]. In terms of its therapeutic efficacy, A2780 ovarian cancer cells treated with conditioned media from the engineered AD-MSCs that were exposed to mild magnetic hyperthermia showed a remarkable decrease in cell viability (40% decrease) when compared to those treated with conditioned media from engineered AD-MSCs controls that had not been exposed to mild magnetic hyperthermia (Fig. 6D).

To confirm that this loss in viability was a function of the mild magnetic hyperthermia-activated secretion of TRAIL from the engineered AD-MSCs, the underlying mechanism was explored. It is well-established that TRAIL primarily induces apoptosis by binding to death receptor 4 (DR4) and death receptor 5 (DR5), which we confirmed to be expressed in A2780 ovarian cancer cells via qPCR (Fig. S8A) [45]. As such, we first investigated the contribution of the death receptors to the observed decrease in cell viability by treating the A2780 cells with monoclonal antibodies blocking DR4 and/or DR5 selectively prior to exposure to conditioned media from the engineered AD-MSCs that were exposed to mild magnetic hyperthermia. We found that blocking DR4 alone (82.7% cell viability), DR5 alone (75.7% cell viability), and both DR4 and DR5 (87.7% cell viability) were able to abrogate the effect of the conditioned media (Fig. S8B). This agrees with our qPCR (Fig. S8A) and previous results from the literature [46,47], which show/state that DR4 is expressed at higher levels than DR5. Moreover, upon immunodepletion of TRAIL from conditioned media of engineered AD-MSCs that were exposed to mild

magnetic hyperthermia using magnetic nanoparticles functionalized with anti-TRAIL antibody, it was observed that the apoptotic effect of the AD-MSC conditioned media was reversed (90.1% cell viability). Next, as it has been reported that TRAIL acts primarily through the activation of caspase-8 and subsequent activation of caspase-3 [48], we confirmed that A2780 ovarian cancer cells that have been exposed to conditioned media from the engineered AD-MSCs that were exposed to mild magnetic hyperthermia exhibited significant activation of caspases when compared to those treated with conditioned media from engineered AD-MSCs controls that had not been exposed to mild magnetic hyperthermia (Fig. 6E). Lastly, we demonstrated that specific inhibition of caspase-8 (85.2% cell viability) and non-specific inhibition of caspases (97.9% cell viability) were able to neutralize the effect of the conditioned media (Fig. S8C). As such, these results confirm that the observed decrease in A2780 cell viability is due to the mild magnetic hyperthermia-activated secretion of TRAIL from the engineered AD-MSCs.

Finally, we have also conducted *in vivo* studies, wherein engineered AD-MSCs were delivered into a metastatic ovarian cancer mouse model via i.p. injection. Our results suggest that engineered AD-MSCs, which secrete TRAIL, are efficacious and can significantly decrease tumor volume when compared to unengineered AD-MSC controls as well as treatment with a single dose of recombinant TRAIL (5 mg/kg via i.p. injection) over a two-week period (Fig. 6F and S9). Specifically, we found that even after a single dose of half a million engineered AD-MSCS (sTRAIL-EGFP plasmid), the overall tumor volume, as measured by luminescence intensity, decreased by over 50% (Fig. 6G). On the other hand, treatment with a single dose of recombinant TRAIL (5 mg/kg) did not decrease tumor size. Instead, the size of the tumor in mice that were treated with a single dose of recombinant TRAIL remained nearly constant over the two-week period. This agrees with previous reports from the literature as recombinant TRAIL is limited by its short half-life. As such, treatment with recombinant TRAIL typically requires high doses (1–10 mg/kg) that are injected daily [49].

4. Conclusions

In this work, a stimuli-responsive stem cell-based gene therapy was developed to enhance the treatment of ovarian cancer. In particular, MCNPs were used for the dual purpose of delivering a heat-inducible plasmid encoding TRAIL and remotely activating TRAIL secretion in the engineered AD-MSCs via mild magnetic hyperthermia. As such, by combining the tumor tropism of the AD-MSCs with the spatiotemporal MCNP-based delivery and activation of TRAIL expression, this platform provides an attractive means with which to enhance our control over the activation of stem cell-based gene therapies. Importantly, we demonstrated that the process of engineering the AD-MSCs did not significantly affect their innate proliferation, differentiation, and tumor homing capabilities. Moreover, mild magnetic hyperthermia resulted in the selective expression of TRAIL in the engineered MSCs, thereby inducing significant ovarian cancer cell apoptosis and death *in vitro* and *in vivo*.

Previous studies have demonstrated that mild hyperthermia can be used to activate genes [50–53]. However, these reports have primarily focused on simple proof-of-concept studies wherein reporter genes were activated in cancer cells. For instance, Ortnier et al. used iron oxide nanoparticles to deliver a heat-inducible luciferase or GFP plasmid to Human embryonic kidney 293 (HEK293) cells [51]. In particular, they demonstrated that they could regulate reporter gene expression *in vitro* using magnetic hyperthermia. On the other hand, Yamaguchi et al. demonstrated a heat-inducible system for cancer treatment, wherein magnetic

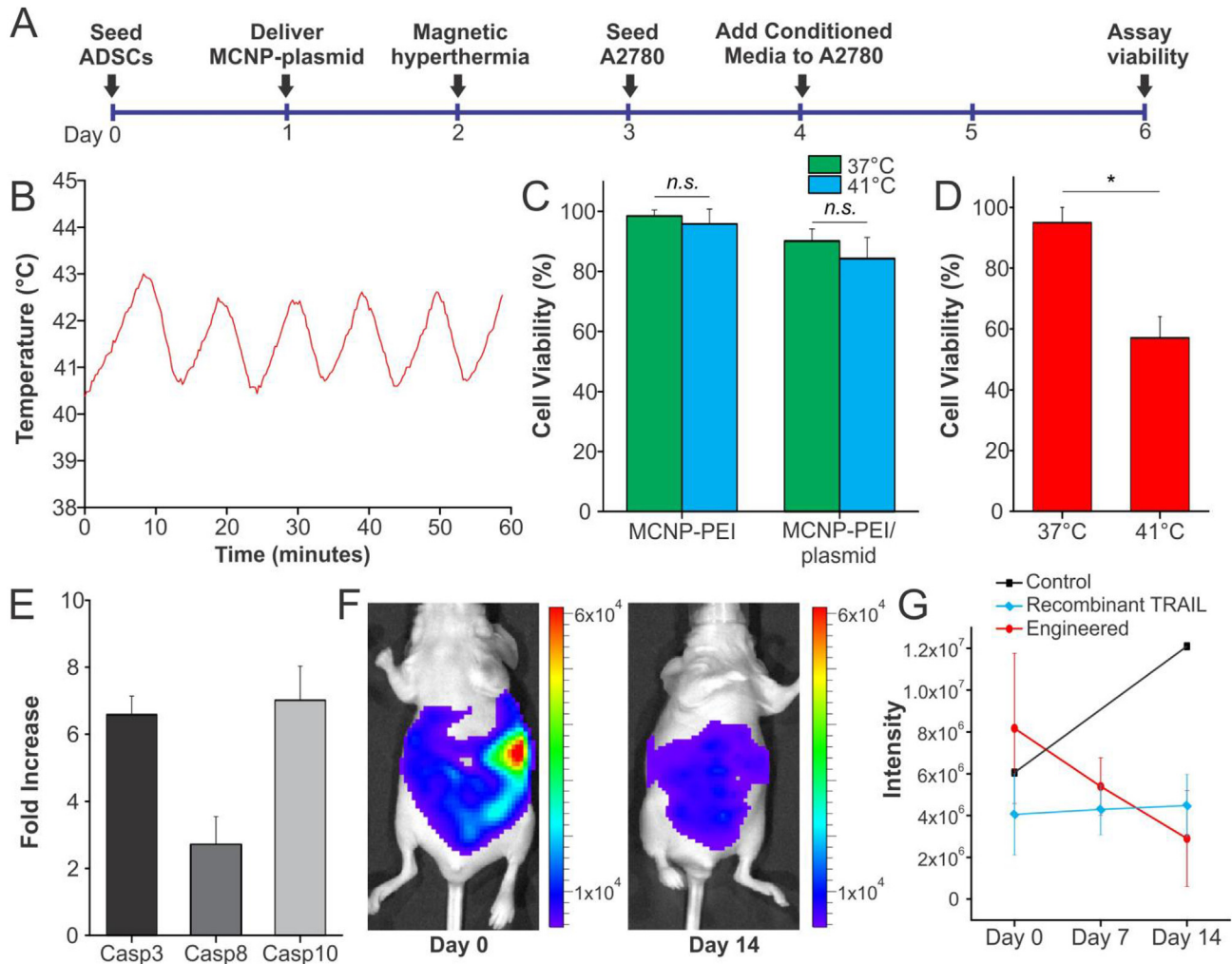


Fig. 6. Engineered AD-MSCs Can Effectively Induce Apoptosis When Exposed to Heat. A) Timeline of the *in vitro* study. B) Mild magnetic hyperthermia with an average temperature of 41.5 °C was maintained for 1 h by periodically exposing the engineered AD-MSCs to an AMF (5 min on, 5 min off). C) Mild magnetic hyperthermia alone did not significantly affect AD-MSC viability. Moreover, the process of engineering the AD-MSCs with MCNP-PEI/plasmid complexes did not significantly affect cell viability. D) To test therapeutic efficacy, A2780 ovarian cancer cells were treated with conditioned media from the engineered AD-MSCs that were exposed to mild magnetic hyperthermia. A2780 cells showed a remarkable decrease in cell viability when compared to those treated with conditioned media from engineered AD-MSCs that had not been exposed to mild magnetic. E) To confirm the mechanism of action, qPCR for caspases, which are downstream of TRAIL, was performed. F) To evaluate *in vivo* efficacy, we injected half a million AD-MSCS engineered with MCNP-PEI/plasmid complex, wherein the plasmid was sTRAIL-EGFP. Unengineered AD-MSCs and a single dose of recombinant TRAIL (5 mg/kg) were injected as controls. Tumor volume was followed over two weeks, we found that the size of the tumors decreased significantly (max value at day 0 was 6×10^4 whereas the max value on day 14 was 8×10^3) when treated with the engineered AD-MSCs. G) Quantification of luminescence intensity shows that the engineered AD-MSCs are significantly better than treatment with a single dose of recombinant TRAIL.

nanoparticles were used to deliver a heat-inducible plasmid encoding tumor necrosis factor alpha (TNF- α) [50]. In this case, these magnetic nanoparticle–plasmid complexes were delivered directly to the human lung adenocarcinoma cells (A549) in order to induce apoptosis of the lung adenocarcinoma cells. Using this system, the authors were able to control the expression of TNF- α in the transfected cancer cells both *in vitro* and *in vivo* using magnetic hyperthermia, thereby demonstrating a local and effective cancer therapy.

While promising, these previous demonstrations are still plagued by the difficulty of actually delivering the magnetic nanoparticles and plasmids to the tumor *in vivo*. As such, they would be unable to target cancers in distinct parts of the body where the cancer has metastasized and, as a result, would be extremely difficult to translate to the clinic. Moreover, the cell lines used in these previous studies are relatively easy to transfect. Addressing these challenges, we have demonstrated an advanced heat-activated gene therapies in this report, wherein we

engineered stem cells in order to take advantage of their innate tumor targeting ability. In particular, we are the first to report the use of mild magnetic hyperthermia to remotely activate a heat-inducible gene in stem cells. In the future, we envision that the biocompatible mSi shell of the MCNP can be filled with chemotherapy in order to enhance the effect of TRAIL. For instance, while the delivery of TRAIL has already been shown to be effective against cancer cells that have acquired resistance to conventional chemotherapy via p53 inactivation, tumor cells have also developed various mechanisms to escape TRAIL-induced apoptosis [1]. To this end, a number of studies have identified novel combinations that could be used with TRAIL to potentiate its therapeutic efficacy. For instance, Kelly et al. has demonstrated that the pretreatment of prostate cancer cells with doxorubicin can increase their sensitivity to TRAIL [54].

In conclusion, we have successfully combined synthetic biology with nanotechnology, wherein mild magnetic hyperthermia was used to specifically activate genes in stem cells. Owing to the great

potential of stem cells, the implications of this study go well beyond cancer applications, and can potentially be used for a host of applications that range from the stimuli-guided differentiation of stem cells for the treatment of injuries such as spinal cord or traumatic brain injury to other diseases such as those involving inflammation, wherein stem cells can be engineered to conditionally secrete anti-inflammatory molecules. As such, we have demonstrated a stimuli-responsive stem cell-based gene therapy using multifunctional MCNPs, which could have great potential for both cancer and other regenerative applications.

Acknowledgments

We would like to acknowledge Drs. Leaf Huang (Department of Biomedical Engineering, University of North Carolina at Chapel Hill) and Yukai He (Cancer Center, Georgia Health Sciences University) for graciously providing us with the plasmid that encodes the recombinant TRAIL. The work was supported by the NIH Director's Innovator Award [1DP20D006462-01], the National Institute of Neurological Disorders and Stroke (NINDS) [R21NS0855691], the National Cancer Institute (NCI) [R01CA138533], and the N.J. Commission on Spinal Cord grant [CSCR13ERG005]. P.T.Y. would also like to acknowledge the National Institutes of Health under Ruth L. Kirschstein National Research Service Award T32 GM8339 from the NIGMS. Finally, S.S. acknowledges the NSF DGE 0801620, Integrative Graduate Education and Research Traineeship (IGERT) on the Integrated Science and Engineering of Stem Cells.

Appendix A. Supplementary data

Supplementary data related to this article can be found at <http://dx.doi.org/10.1016/j.biomaterials.2015.11.023>.

References

- [1] N.G. Khaider, D. Lane, I. Matte, C. Rancourt, A. Piche, Targeted ovarian cancer treatment: the TRAILs of resistance, *Am. J. Cancer Res.* 2 (2012) 75–92.
- [2] K.S. Bevis, D.J. Buchsbaum, J.M. Straughn, Overcoming TRAIL resistance in ovarian carcinoma, *Gynecol. Oncol.* 119 (2010) 157–163.
- [3] G.D. Aletti, M.M. Gallenberg, W.A. Cliby, A. Jatoi, L.C. Hartmann, Current management strategies for ovarian cancer, *Mayo Clin. Proc.* 82 (2007) 751–770.
- [4] W.P. McGuire, W.J. Hoskins, M.F. Brady, P.R. Kucera, E.E. Partridge, K.Y. Look, et al., Cyclophosphamide and cisplatin compared with paclitaxel and cisplatin in patients with stage III and stage IV ovarian cancer, *New Engl. J. Med.* 334 (1996) 1–6.
- [5] D. Peer, J.M. Karp, S. Hong, O.C. FaroKHzad, R. Margalit, R. Langer, Nanocarriers as an emerging platform for cancer therapy, *Nat. Nanotechnol.* 2 (2007) 751–760.
- [6] M.F. Pittenger, A.M. Mackay, S.C. Beck, R.K. Jaiswal, R. Douglas, J.D. Mosca, et al., Multilineage potential of adult human mesenchymal stem cells, *Science* 284 (1999) 143–147.
- [7] E.L. Spaeth, F.C. Marini, Dissecting mesenchymal stem cell movement: migration assays for tracing and deducing cell migration, *Methods Mol. Biol.* 750 (2011) 241–259.
- [8] A.L. Ponte, E. Marais, N. Gallay, A. Langonne, B. Delorme, O. Herault, et al., The in vitro migration capacity of human bone marrow mesenchymal stem cells: comparison of chemokine and growth factor chemotactic activities, *Stem cells* 25 (2007) 1737–1745.
- [9] H. Yagi, A. Soto-Gutierrez, B. Parekhdan, Y. Kitagawa, R.G. Tompkins, N. Kobayashi, et al., Mesenchymal stem cells: mechanisms of immunomodulation and homing, *Cell Transpl.* 19 (2010) 667–679.
- [10] S.B. Coffelt, F.C. Marini, K. Watson, K.J. Zvezdaryk, J.L. Dembinski, H.L. LaMarca, et al., The pro-inflammatory peptide LL-37 promotes ovarian tumor progression through recruitment of multipotent mesenchymal stromal cells, *Proc. Natl. Acad. Sci. U. S. A.* 106 (2009) 3806–3811.
- [11] Z.B. Gao, L.N. Zhang, J. Hu, Y.J. Sun, Mesenchymal stem cells: a potential targeted-delivery vehicle for anti-cancer drug, loaded nanoparticles, *Nanomed. Nanotechnol.* 9 (2013) 174–184.
- [12] R.M. Dwyer, S. Khan, F.P. Barry, T. O'Brien, M.J. Kerin, Advances in mesenchymal stem cell-mediated gene therapy for cancer, *Stem Cell Res. Ther.* 1 (2010).
- [13] X. Ling, F. Marini, M. Konopleva, W. Schober, Y. Shi, J. Burks, et al., Mesenchymal stem cells overexpressing IFN-beta inhibit breast cancer growth and metastases through Stat3 signaling in a syngeneic tumor model, *Cancer Microenviron. Off. J. Int. Cancer Microenviron. Soc.* 3 (2010) 83–95.
- [14] M.R. Loebinger, A. Eddaoudi, D. Davies, S.M. Janes, Mesenchymal stem cell delivery of TRAIL can eliminate metastatic cancer, *Cancer Res.* 69 (2009) 4134–4142.
- [15] M. Ehtesham, P. Kabos, A. Kabosova, T. Neuman, K.L. Black, J.S. Yu, The use of interleukin 12-secreting neural stem cells for the treatment of intracranial glioma, *Cancer Res.* 62 (2002) 5657–5663.
- [16] H. Walczak, R.E. Miller, K. Ariail, B. Gliniak, T.S. Griffith, M. Kubin, et al., Tumoricidal activity of tumor necrosis factor related apoptosis-inducing ligand in vivo, *Nat. Med.* 5 (1999) 157–163.
- [17] L.P. Mueller, J. Luetzendorf, M. Widder, K. Nerger, H. Caysa, T. Mueller, TRAIL-transduced multipotent mesenchymal stromal cells (TRAIL-MS-C) overcome TRAIL resistance in selected CRC cell lines in vitro and in vivo, *Cancer Gene Ther.* 18 (2011) 229–239.
- [18] X. Volkman, U. Fischer, M.J. Bahr, M. Ott, F. Lehner, M. MacFarlane, et al., Increased hepatotoxicity of tumor necrosis factor-related apoptosis-inducing ligand in diseased human liver, *Hepatology* 46 (2007) 1498–1508.
- [19] D. Lawrence, Z. Shahrokh, S. Marsters, K. Achilles, D. Shih, B. Mounho, et al., Differential hepatocyte toxicity of recombinant Apo2L/TRAIL versions, *Nat. Med.* 7 (2001) 383–385.
- [20] S. Rohmer, A. Mainka, I. Knippertz, A. Hesse, D.M. Nettelbeck, Insulated hsp70B' promoter: stringent heat-inducible activity in replication-deficient, but not replication-competent adenoviruses, *J. Gene Med.* 10 (2008) 340–354.
- [21] P.T. Yin, B.P. Shah, K.B. Lee, Combined magnetic nanoparticle-based microRNA and hyperthermia therapy to enhance apoptosis in brain cancer cells, *Small* 10 (2014) 4106–4112.
- [22] B.P. Shah, N. Pasquale, G.J. De, T. Tan, J.J. Ma, K.B. Lee, Core-shell nanoparticle-based peptide therapeutics and combined hyperthermia for enhanced cancer cell apoptosis, *ACS Nano* 8 (2014) 9379–9387.
- [23] B. Shah, P.T. Yin, S. Ghoshal, K.B. Lee, Multimodal magnetic core-shell Nanoparticles for effective stem-cell differentiation and imaging, *Angew. Chem. Int. Ed.* 52 (2013) 6190–6195.
- [24] S. Sun, H. Zeng, D.B. Robinson, S. Raoux, P.M. Rice, S.X. Wang, et al., Monodisperse MFe₂O₄ (M = Fe, Co, Mn) nanoparticles, *J. Am. Chem. Soc.* 126 (2004) 273–279.
- [25] J.T. Jang, H. Nah, J.H. Lee, S.H. Moon, M.G. Kim, J. Cheon, Critical enhancements of MRI contrast and hyperthermic effects by dopant-controlled magnetic nanoparticles, *Angew. Chem. Int. Ed.* 48 (2009) 1234–1238.
- [26] J. Kim, H.S. Kim, N. Lee, T. Kim, H. Kim, T. Yu, et al., Multifunctional uniform nanoparticles composed of a magnetite nanocrystal core and a mesoporous silica shell for magnetic resonance and fluorescence imaging and for drug delivery, *Angew. Chem. Int. Ed.* 47 (2008) 8438–8441.
- [27] M. Kallumadil, M. Tada, T. Nakagawa, M. Abe, P. Southern, Q.A. Pankhurst, Suitability of commercial colloids for magnetic hyperthermia, *J. Magn. Magn. Mater.* 321 (2009) 1509–1513.
- [28] X. Wu, Y. He, L.D. Faló Jr., K.M. Hui, L. Huang, Regression of human mammary adenocarcinoma by systemic administration of a recombinant gene encoding the hFlex-TRAIL fusion protein, *Mol. Ther.* 3 (2001) 368–374.
- [29] J. Hageman, H.H. Kampinga, Computational analysis of the human HSPH/HSPA/DNAJ family and cloning of a human HSPH/HSPA/DNAJ expression library, *Cell Stress Chaperon* 14 (2009) 1–21.
- [30] O. Boussif, F. Lezoualch, M.A. Zanta, M.D. Mergny, D. Scherman, B. Demeneix, et al., A versatile vector for gene and oligonucleotide transfer into cells in culture and in-vivo – polyethylenimine, *Proc. Natl. Acad. Sci. U. S. A.* 92 (1995) 7297–7301.
- [31] B. Urban-Klein, S. Werth, S. Abuharbeid, F. Czubayko, A. Aigner, RNAi-mediated gene-targeting through systemic application of polyethylenimine (PEI)-complexed siRNA in vivo, *Gene Ther.* 12 (2005) 461–466.
- [32] I.A. Baber, C.J. Cheng, C.J. Booth, X.P. Liang, J.B. Weidhaas, W.M. Saltzman, et al., Nanoparticle-based therapy in an in vivo microRNA-155 (miR-155)-dependent mouse model of lymphoma, *Proc. Natl. Acad. Sci. U. S. A.* 109 (2012) E1695–E1704.
- [33] J.P. Behr, The proton sponge: a trick to enter cells the viruses did not exploit, *Chimia* 51 (1997) 34–36.
- [34] S. Hobe, A. Aigner, Polyethylenimines for siRNA and miRNA delivery in vivo, *Wires Nanomed. Nanobiot.* 5 (2013) 484–501.
- [35] R. Savla, O.B. Garbuzenko, S. Chen, L. Rodriguez-Rodriguez, T. Minko, Tumor-targeted responsive nanoparticle-based systems for magnetic resonance imaging and therapy, *Pharm. Res.* 31 (2014) 3487–3502.
- [36] M. Zhang, O.B. Garbuzenko, K.R. Reuhl, L. Rodriguez-Rodriguez, T. Minko, Two-in-one: combined targeted chemo and gene therapy for tumor suppression and prevention of metastases, *Nanomedicine Lond.* 7 (2012) 185–197.
- [37] Y. Liu, M.K. Shipton, J. Ryan, E.D. Kaufman, S. Franzen, D.L. Feldheim, Synthesis, stability, and cellular internalization of gold nanoparticles containing mixed peptide-poly(ethylene glycol) monolayers, *Anal. Chem.* 79 (2007) 2221–2229.
- [38] E. Delyagina, A. Schade, D. Scharfenberg, A. Skorska, C. Lux, W.Z. Li, et al., Improved transfection in human mesenchymal stem cells: effective intracellular release of pDNA by magnetic polyplexes, *Nanomedicine UK* 9 (2014) 999–1017.
- [39] P.M. Zelis, G.A. Pasquevich, S.J. Stewart, M.B.F. van Raap, J. Apesteguy, I.J. Bruvera, et al., Structural and magnetic study of zinc-doped magnetite nanoparticles and ferrofluids for hyperthermia applications, *J. Phys. D. Appl.*

- Phys. 46 (2013).
- [40] E.J. Noonan, R.F. Place, C. Giardina, L.E. Hightower, Hsp70B' regulation and function, *Cell Stress Chaperon* 12 (2007) 219–229.
- [41] H.R. Kohler, B. Rahman, S. Graff, M. Berkus, R. Triebksorn, Expression of the stress-70 protein family (HSP70) due to heavy metal contamination in the slug, *deroceras reticulatum*: an approach to monitor sublethal stress conditions, *Chemosphere* 33 (1996) 1327–1340.
- [42] H.K. Salem, C. Thiemermann, Mesenchymal stromal cells: current understanding and clinical status, *Stem Cells* 28 (2010) 585–596.
- [43] T.-H. Kim, S. Shah, L. Yang, P.T. Yin, M.K. Hossain, B. Conley, et al., Controlling differentiation of adipose-derived stem cells using combinatorial graphene hybrid-pattern arrays, *ACS Nano* 9 (2015) 3780–3790.
- [44] Y. Reissis, E. Garcia-Gareta, M. Korda, G.W. Blunn, J. Hua, The effect of temperature on the viability of human mesenchymal stem cells, *Stem Cell Res. Ther.* 4 (2013) 139.
- [45] R.W. Johnstone, A.J. Frew, M.J. Smyth, The TRAIL apoptotic pathway in cancer onset, progression and therapy, *Nat. Rev. Cancer* 8 (2008) 782–798.
- [46] B.M. Kurbanov, C.C. Geilen, L.F. Fecker, C.E. Orfanos, J. Eberle, Efficient TRAIL-R1/DR4-mediated apoptosis in melanoma cells by tumor necrosis factor-related apoptosis-inducing ligand (TRAIL), *J. Investig. Dermatol.* 125 (2005) 1010–1019.
- [47] H.J. Arts, S. de Jong, H. Hollema, K. ten Hoor, A.G. van der Zee, E.G. de Vries, Chemotherapy induces death receptor 5 in epithelial ovarian carcinoma, *Gynecol. Oncol.* 92 (2004) 794–800.
- [48] Y. Deng, Y. Lin, X. Wu, TRAIL-induced apoptosis requires Bax-dependent mitochondrial release of Smac/DIABLO, *Genes Dev.* 16 (2002) 33–45.
- [49] A. Ashkenazi, R.C. Pai, S. Fong, S. Leung, D.A. Lawrence, S.A. Marsters, et al., Safety and antitumor activity of recombinant soluble Apo2 ligand, *J. Clin. Investig.* 104 (1999) 155–162.
- [50] M. Yamaguchi, A. Ito, A. Ono, Y. Kawabe, M. Kamihira, Heat-inducible gene expression system by applying alternating magnetic field to magnetic nanoparticles, *ACS Synth. Biol.* 3 (2014) 273–279.
- [51] V. Ortner, C. Kaspar, C. Halter, L. Tollner, O. Mykhaylyk, J. Walzer, et al., Magnetic field-controlled gene expression in encapsulated cells, *J. Control Release* 158 (2012) 424–432.
- [52] Q-s Tang, D-s Zhang, X-m Cong, M-l Wan, L-q jin, Using thermal energy produced by irradiation of Mn–Zn ferrite magnetic nanoparticles (MZF-NPs) for heat-inducible gene expression, *Biomaterials* 29 (2008) 2673–2679.
- [53] A. Ito, M. Shinkai, H. Honda, T. Kobayashi, Heat-inducible TNF-alpha gene therapy combined with hyperthermia using magnetic nanoparticles as a novel tumor-targeted therapy, *Cancer Gene Ther.* 8 (2001) 649–654.
- [54] M.M. Kelly, B.D. Hoel, C. Voelkel-Johnson, Doxorubicin pretreatment sensitizes prostate cancer cell lines to TRAIL induced apoptosis which correlates with the loss of c-FLIP expression, *Cancer Biol. Ther.* 1 (2002) 520–527.